

Non-Gaussian state teleportation with a nonlinear feedforward

Vojtěch Kala¹, Mattia Walschaers², Radim Filip¹, and Petr Marek¹

¹ Department of Optics, Palacký University, 17. listopadu 1192/12, 77146 Olomouc, Czech Republic

² Laboratoire Kastler Brossel, Sorbonne Université, CNRS, ENS-PSL Research University, Collège de France; 4 place Jussieu, F-75252 Paris, France

Measurement-induced quantum computation with continuous-variable cluster states utilizes teleportation propagating the states through the cluster accompanied by non-Gaussian measurements and feedforward control. We analyze such propagation of a quantum non-Gaussian state with nonlinear squeezing through a small cluster state and show that when a nonlinear feedforward is involved in the teleportation protocol, higher nonlinear squeezing can be transferred. In a probabilistic regime, the improvement can be manifested even with current experimental resources. Better processing of non-Gaussian states can bring us closer to the necessary interplay between cluster states and non-Gaussianity required by quantum computing.

1 Introduction

Entangled Gaussian cluster states offer a rich multimode structure. Accompanied by single photon measurements, their simulation complexity exceeds the abilities of classical computation [5, 12]. Their capacity for massive multi-mode multiplexing [22, 28, 32, 48] is the main advantage of measurement-induced quantum computing with bosonic modes of traveling light. In this protocol, measurements of the individual modes enable the quantum information to propagate along the cluster and evolve in the desired manner [28, 29, 47]. The choice of measurement is what determines whether the state is simply transmitted by quantum teleportation [2, 8, 35, 41, 47] or transformed [7, 13, 31, 37]. To reach the full advantages of the quantum computation, the Gaussian entangled states need to be further supported by deterministic non-Gaussian operations [5, 11, 25, 26]. These challenging operations can be implemented in a measurement-induced fashion, [18, 31] leaving it with two distinct tasks: experimental generation of the non-Gaussian states, and successful propagation of the non-Gaussian states through a Gaussian circuit.

In quantum optics with traveling light, non-Gaussian quantum states have been generated in a wide range of experimental configurations [21, 33, 34, 44, 49, 50]. Today, photon-number-resolving detectors, together with Gaussian operations such as parametric down-conversion and coherent classical displacements, are feasibly used to probabilistically generate non-Gaussian states with varied nonclassical and non-Gaussian properties

Vojtěch Kala: kala@optics.upol.cz

Mattia Walschaers: mattia.walschaers@lkb.upmc.fr

Radim Filip: filip@optics.upol.cz

Petr Marek: marek@optics.upol.cz

[1, 19, 20, 27, 42, 43]. One of these important properties is the nonlinear squeezing that can be used as a resource for deterministic preparation of cubic nonlinearity [31, 36] and is a specific example of a purely continuous non-Gaussian resource [17, 19, 45]. The basic principle of the state preparation, closely aligned to the Gaussian boson sampling problem [12], is still actively investigated to prepare more and more complex quantum states [39]. The successful generation of non-Gaussian states led to their active use in tests of their propagation through Gaussian circuits, resulting in demonstration of key protocols, such as teleportation [3, 9, 15, 23, 30, 40, 51], decoherence prevention [16], or nonlinear measurement [36]. One thing shared by all of these experimental tests is that the non-Gaussian features of the employed states are deteriorated in the process, diminishing their power. Therefore, novel ways of processing that help preserve the non-Gaussianity will be needed while moving forward.

In this paper we are going to show how the canonical teleportation protocol along a single node of an entangled cluster can be enhanced by a classical non-linear feedforward to better transfer a specific class of non-Gaussian quantum states. We focus on quantum states with cubic nonlinear squeezing which is a resource for measurement-based quantum computation with continuous variables. To this end we are going to consider the problem of teleporting these states, substantially different than Fock states, qubit states and cat states, and compare the canonical teleportation to the teleportation with enhanced feedforward operation. In the field of measurement-induced operations, the teleportation of a state with nonlinear squeezing enriched by nonlinear feedforward can be seen as an approximation of the cubic nonlinear phase measurement [36]. The teleported state serves as an ancillary state and together with the homodyne measurements and feedforward they construct the approximated measurement which applies to the first mode of the two-mode Gaussian state. Therefore, our analyses will also test the projection powers of the approximate measurement as a state preparation. We are going to compare this approximation to the ultimate ideal theoretical bound provided by the ideal cubic measurement.

2 Teleportation, linear and nonlinear

2.1 Deterministic regime

The teleportation protocol [8, 35] is the basic building block of the cluster state computing. The usual involved measurement is the homodyne detection with a linear feedforward that provides linear dependence of operations performed on the outcoming state on measurements results. It is possible to consider also generalized measurement, that enables not only transfer of quantum states but also their transformation. Such a measurement can include adjustable nonlinear feedforward that utilizes the measurement results in some more complex function.

A single step of the transfer, the canonical teleportation protocol itself, is schematically depicted in Fig. 1a. Within the protocol, the initial state in mode Q interacts on a balanced beam splitter with mode A of a two-mode entangled state and the two resulting modes are measured by a pair of homodyne detectors. The measured values are then used for the feedforward displacement operation on the remaining mode B of the entangled state, leaving its quadrature operators transformed as

$$\begin{aligned} x_B^{\text{out}} &= x_Q + x_B - x_A = x_Q + N_x \\ p_B^{\text{out}} &= p_Q + p_A + p_B = p_Q + N_p. \end{aligned} \tag{1}$$

The expressions used for individual transformations generated by beam splitter and other optical elements can be found in Appendix A. Quadratures x and p of the optical field obey

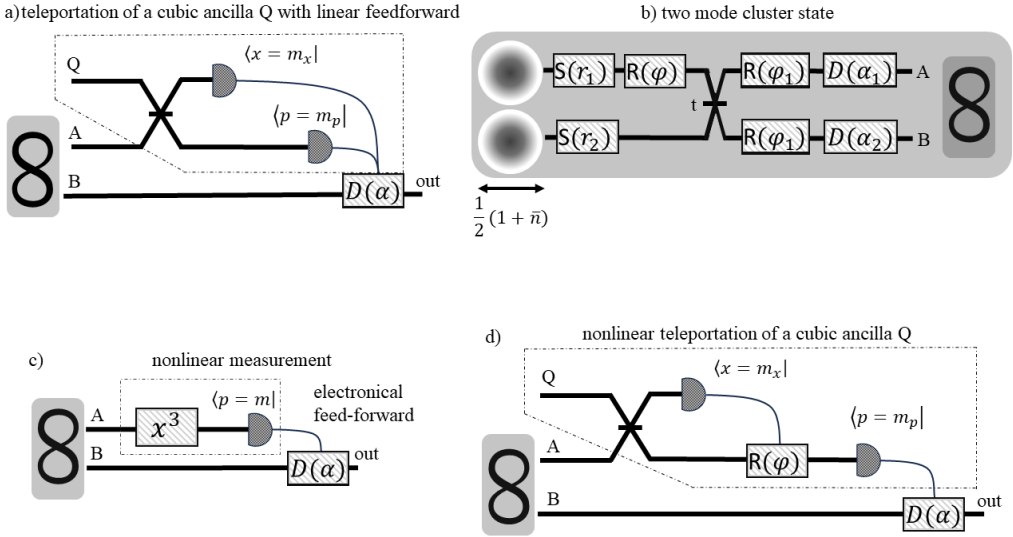


Figure 1: a) Regular teleportation scheme transferring the quantum state through the cluster state. b) Optical scheme equivalent to parameterization of the cluster state considered for the analyzed schemes. c) Optical scheme showing the nonlinear cubic phase measurement applied to one part of the cluster state. The measurement is decomposed into an ideal cubic nonlinearity followed by homodyne measurement. The measurement result is used in a feedforwarded displacement on the second mode. d) Nonlinear teleportation with nonlinear feedforward and ancillary state in the mode Q.

$[x, p] = i$. The statistics of the teleported state is accompanied by noise terms N_x and N_p , that depend on the properties of the two-mode entangled state, illustrated in Fig. 1b, and vanish for the ideal EPR state with maximal correlation and infinite energy. Despite the protocol yielding perfect results in the limit of infinite squeezing, the real performance will always be noisy, with an imperfect outcome.

Our goal is teleportation of a quantum non-Gaussian state. Specifically the cubic phase state

$$|\chi\rangle = C(\chi)S(r)|0\rangle, \quad (2)$$

where $|p = 0\rangle$ is an eigenstate of the p quadrature with eigenvalue 0. In this case, the teleportation can be seen as similar to remote state preparation, which could be best achieved by measuring one of the entangled modes in a correct basis. The projection on a cubic state can be performed by the ideal cubic measurement [36], illustrated in Fig. 1c. POVM element of the measurement can be expressed as

$$\Pi = C(\chi)|p = m\rangle\langle p = m|C(\chi)^\dagger, \quad (3)$$

where

$$C(\chi) = \exp\left(-i\chi\frac{x^3}{3}\right), \quad (4)$$

is the cubic nonlinearity and $|p = m\rangle$ is an eigenstate of the p quadrature with eigenvalue m . In the ideal scenario, the measurement can be understood as measurement of nonlinear combination of quadrature operators

$$O = p + zx^2, \quad (5)$$

that projects on its eigenstates. Such states have infinite energy, similar to position eigenstates, which are projected on by homodyne measurement [10, 11]. The measurement can

be decomposed into the cubic nonlinearity and p-homodyne measurement. These operations can be sequentially applied to one part of the two-mode cluster state as is shown in Fig. 1c. It is necessary to utilize the measurement result m in a Gaussian feedforward in order to obtain a non-Gaussian state. If the measurement outcome is disregarded, the outcoming state is quantum Gaussian, i.e. it is a mixture of Gaussian states. In Heisenberg picture, the overall transformation yields

$$\begin{aligned} x_B^{\text{out}} &= x_B \\ p_B^{\text{out}} &= p_B + g_p p_A + g_p \chi x_A^2. \end{aligned} \quad (6)$$

Here the output is displaced in p over the measurement result with gain g_p . Note the appearance of nonlinear terms that originates from the cubic nonlinearity, which action is in more detail described in Appendix A.

In an experimentally realistic scenario, we can substitute the cubic nonlinearity by its measurement-induced version and arrive at the scheme for nonlinear teleportation as is shown in Fig. 1d. The ideal cubic nonlinearity (4) can be approximated for traveling beams of light by a Gaussian circuit supported by non-Gaussian ancillary state and equipped with electronical nonlinear feedforward of the measurement results, see Fig. 1d [31, 36]. The first arm of the bipartite Gaussian state interferes with an ancillary state on a beam splitter. The result of its x -homodyne measurement m_x is used in a nonlinear feedforward for a phase shift $\phi = \text{atan}(\sqrt{2}\chi m_x)$ applied to the remaining mode followed by p-homodyne detection. Both measurement results are eventually used to compute the required displacement on the unmeasured mode. Using this circuit, we can asymptotically approach the ideal measurement in Fig. 1b. The generated transformation of quadratures is in structure similar to the one produced by the regular teleportation

$$\begin{aligned} x_B^{\text{out}} &= x_Q + N_x \\ p_B^{\text{out}} &= p'_Q + N'_p. \end{aligned} \quad (7)$$

Whereas the noise term N_x remains the same as in the case of regular teleportation, new nonlinear terms appear in transformation of the p quadrature

$$\begin{aligned} N'_p &= p_B + p_A + \frac{\chi}{2} x_A^2 \\ p'_Q &= p_Q - \frac{\chi}{2} x_Q^2. \end{aligned} \quad (8)$$

Therefore, the p_Q quadrature of the ancillary mode Q that initially carries the nonlinear squeezing is nonlinearly transformed and accompanied by non-Gaussian noise terms.

We further generalize the gains and transmissivity of the beam splitter in the nonlinear teleportation scheme which changes the formulas to

$$\begin{aligned} x_B^{\text{out}} &= x_B + d_F(tx_Q - rx_A) \\ p_B^{\text{out}} &= p_B + g_F \cos(\theta)(tp_A + rp_Q + \sqrt{2}\chi(tx_A + rx_Q)(rx_A - tx_Q)), \end{aligned} \quad (9)$$

with d_F and g_F being electronic gains, and t and r being the transmissivity and reflectivity of the beam splitter before the homodyne measurements. By setting $\chi = 0$, the equation (9) describes the regular teleportation with generalized gains and beam splitter transmissivity.

2.2 Probabilistic regime

Schemes described in the previous subsection work in the deterministic regime, accepting all measurement results and processing them in the feedforward. Different measurement

results of the homodyne measurements m_x and m_p can generally lead to a different quantum states $\hat{\rho}(m_x, m_p)$

$$\hat{\rho}(m_x, m_p) = \frac{\text{Tr}_{AB}[\rho_{ABQ}\Pi(m_x, m_p)]}{\text{Tr}[\rho_{ABQ}\Pi(m_x, m_p)]}. \quad (10)$$

Here ρ_{ABQ} is the density matrix of the cluster state and ancillary mode and $\Pi(m_x, m_p)$ a POVM element describing the measurement. For the ideal nonlinear measurement shown in Fig. 1c, it is the POVM in (3). For the regular and nonlinear teleportation it yields

$$\Pi(m_x, m_p)_c = U_{BS}(t)^\dagger |x = m_x\rangle_Q \langle x = m_x| \otimes |p = m_p\rangle_A \langle p = m_p| U_{BS}(t) \quad (11)$$

and

$$\Pi(m_x, m_p)_d = U_{BS}(t)^\dagger |x = m_x\rangle_Q \langle x = m_x| \otimes R(\phi(m_x)) |p = m_p\rangle_A \langle p = m_p| R(\phi(m_x)) U_{BS}(t), \quad (12)$$

respectively. The operator $U_{BS}(t)$ is a unitary operation of beam splitter with transmissivity t and $R(\phi(m_x))$ a phase shift over angle depending on the measurement outcome m_x as

$$\phi(m_x) = -\text{atan}(\chi m_x \sqrt{2}). \quad (13)$$

All states $\rho(m_x, m_p)$ contribute to the outcoming mixture

$$\rho_{\text{out}} = \int_r P(m_x, m_p) \rho(m_x, m_p) dm_x dm_p, \quad (14)$$

where the probability is given by

$$P(m_x, m_p) = \text{Tr}_{AB}[\rho_{ABQ}\Pi(m_x, m_p)]. \quad (15)$$

If the integration domain r is the whole phase space, this is the state, whose nonlinear squeezing is computed in the deterministic regime. Generally, the states $\rho(m_x, m_p)$ are different and thus, it can be advantageous to post-select some of them (i.e. choose r as an appropriate subspace of the phase space) in order to increase the nonlinear squeezing at the output. This is, however, accompanied by decreased probability of success.

The analysis is performed in a following way. The density matrices of quantum states are computed for measurement results on a grid in phase space, such that trace of their mixture approaches very closely one. Thus, the grid is sufficiently large to capture all states appearing with numerically significant probability. Then, the states are ordered according to their nonlinear squeezing and aggregated up to some probability P . For this mixture of post-selected states, the nonlinear squeezing is evaluated.

As a preparation of a general two mode Gaussian state is quite complex, we conclude with analysis of a linear unity gain teleportation through a two mode squeezed vacuum compared with the same setup enriched by the nonlinear feedforward. In fact, the nonlinear feedforward can be more complex, also adjusting the outcoming states $\rho(m_x, m_p)$ by Gaussian operations in such a way, that the nonlinear squeezing is maximized for each of the state. This is equivalent to computation of averaged nonlinear squeezing, where not the conditioned states are aggregated, but their nonlinear squeezing

$$\langle \xi(z) \rangle = \int_r P(m_x, m_p) \xi(z)_{\rho(m_x, m_p)} dm_x dm_p. \quad (16)$$

In such a way we present comparison of straightforward scheme of unity gain teleportation through a two mode squeezed vacuum with and without the nonlinear feedforward.

2.3 Nonlinear squeezing

Both the regular and nonlinear teleportation schemes consists of only Gaussian optical elements, therefore, with Gaussian states at the input, the circuit yields classical non-Gaussian mixture of Gaussian states. Any non-Gaussianity of the output state therefore has to originate in the non-Gaussianity of the input state. Our goal here is to look at the teleported state and compute how much of its non-Gaussian properties survived the teleportation

The original role of non-Gaussian ancillary state is to suppress a noise term that appears at the outcome of the measurement-induced cubic phase gate [19, 31]. This term has the same form as the operator (5) that is measured by the nonlinear measurement; the real parameter z is called cubicity. Inspired by insufficiency of Gaussian states for the quantum computing advantage with CV, the nonlinear squeezing is defined as a ratio of variance of the operator O compared to the minimal variance that can be achieved in a Gaussian state [17, 19, 45]

$$\xi(z)_\rho = \frac{\text{var}_\rho(p + zx^2)}{\min_G \text{var}(p + zx^2)}. \quad (17)$$

As a consequence of this definition a state with nonlinear squeezing is certainly non-Gaussian. Our goal, from now on, will be to analyze how well a quantum state with this property can be transferred through a two-mode cluster state. We will specifically look for the maximal nonlinear squeezing attainable at the output of the teleportation protocol with a specific cubic nonlinear state at its input. Subsequently, we will compare this results to the teleportation protocol enhanced by a nonlinear feedforward. Thus, the figure of merit will be the value of the nonlinear squeezing at the output.

The maximal nonlinear squeezing is reached by the unphysical infinite energy cubic state (18). Such a state is well approximated by a cubically transformed squeezed vacuum

$$|\chi\rangle = C(\chi)S(r)|0\rangle. \quad (18)$$

This finitely nonlinearly squeezed state has finite energy and minimizes uncertainty relations. However, it is an idealized approximation in a sense that its preparation still includes experimentally unfeasible cubic nonlinearity.

Experimentally feasible approximations of the finitely nonlinearly squeezed states can be prepared on a finite Fock subspace [14, 49]. The approximations can be written as

$$|\phi_N\rangle = \sum_{n=0}^N c_n |n\rangle, \quad (19)$$

where the coefficients can be found in an efficient way by solving an eigenvalue problem and two variable optimization [31]. Note that Fock states and states with nonlinear squeezing have different symmetries. Unlike the nonlinearly squeezed states that are symmetric in x only, Wigner functions of Fock states are symmetric both in x and p . This difference hints that an approximation of the cubic state must be a superposition of Fock states. The experimentally feasible quantum state exhibiting nonlinear squeezing and simultaneously the lowest order approximation is a superposition of the first two Fock states

$$|\phi_2\rangle = u|0\rangle + i\sqrt{1-u^2}|1\rangle, \quad (20)$$

where u is real and bounded by $0 < u < 1$ [19]. The used parameterization ensures symmetry under transformation $x \rightarrow -x$ which holds also for (5). One step further leads to ancillary state approximation

$$|\phi_3\rangle = c_0|0\rangle + ic_1|1\rangle + c_2|2\rangle, \quad (21)$$

where the c_i are real coefficients. The states can be found as eigenstates of the operator O restricted to an N dimensional subspace of the Fock space. They provide the best nonlinear squeezing available on such a subspace [31].

To show the positive effect of nonlinear feedforward, let us compare the results obtained by the regular and nonlinear teleportation protocols. At the same time, we compare the schemes equipped with identical resources of non-Gaussianity [38] and Gaussian squeezing [4]. The approximations can be classified by the faithful hierarchy of N -photon non-Gaussianity [21] or stellar rank [6]. A superposition (19) with a fixed highest Fock state N has N -photon non-Gaussianity. When teleporting a state with some given N -photon non-Gaussianity and transferring a state from the same level of the hierarchy by nonlinear teleportation, both schemes posses the same N -photon non-Gaussian state and any improvement in performance thus originates from the properties of the scheme. Another resource present in the schemes is Gaussian squeezing [4]. Throughout our analysis we limit the available Gaussian squeezing while comparing the performances. At first in preparation of the finitely squeezed state (18) and as well of the cluster state. We consider a general two-mode Gaussian cluster state, whose parameters are optimized for each situation and each scheme. The optimization is done with help of Python library `scipy optimize` and repeated with randomly chosen initial conditions. Details can be found in Appendix C. To remain close to the experimental reality, we consider an upperbound on Gaussian squeezing available. The optimum is then sought in a range given by these bounds, e.g. ± 9 dB. Overall, by limiting the resources we can perform a genuine comparison of schemes equipped with the same level of N -photon non-Gaussianity and limit on maximal Gaussian squeezing.

The parameterization of the two-mode Gaussian state via the covariance matrix can be found in Appendix B and is equivalent to two thermal states transformed by single mode Gaussian operations and a beam splitter as shown in Fig. 1b. The thermal noise is taken as an input parameter and by its change, we can analyze the resilience of discussed effects. It is described by parameter n representing the multiples of vacuum fluctuations added to an initially pure vacuum state. Thus, for a pure state the parameter yields $n = 0$, while $n > 0$ represents some amount of thermal noise [46].

When processing a quantum state or seeking nonlinear squeezing after a nonlinear measurement on an entangled mode, the nonlinear squeezing of the output state does not need to be minimal for the initial cubicity. Thus we define the native cubicity z_n of a given state ρ as the cubicity for which

$$\xi(z_n)_\rho = \min_z \xi(z)_\rho. \quad (22)$$

The native cubicity z_n , for which the state reveals its maximal nonlinear squeezing, can be considered a property of the state.

3 Results

3.1 Deterministic scheme

The nonlinear squeezing that can be achieved with a pure two-mode cluster state for the individual schemes is shown in Fig. 2 as a function of the maximal available Gaussian squeezing, see appendix B for details. The cluster state is optimized for each scheme with upper bound on Gaussian squeezing and the parameters of the optical circuit are searched to maximize the nonlinear squeezing at the output. Optimized preparation of the cubic state with finite nonlinear squeezing is subject to the same constraints. We also optimize

the coefficients in superpositions (20) and (21) for best performance, thus obtaining states different to the eigenstates of restriction of the O operator on finite Fock subspace.

The plot can be interpreted pairwise, according to the properties of used teleported state and its N -photon non-Gaussianity. This point of view connects together regular teleportation of the state (20) consisting of superposition of vacuum and single photon, and the nonlinear teleportation of the same state (albeit with different optimal coefficient u). Similarly we can compare the regular and nonlinear teleportation for ancillary state (21) and at last the schemes utilizing finitely squeezed cubic state (18). Such approach connects schemes possessing the same resources of non-Gaussianity and Gaussian squeezing with differences only in the classical part that processes measurement results and governs feedforwarded Gaussian operations.

Teleportation of the weak nonlinear effects provided by the two component ancillary state (20) shows the strength of linear Gaussian processing as the nonlinear feedforward introduces no significant improvement in deterministic regime. When increasing the resource to two-photon non-Gaussianity (21) there is a slight difference for a realistic Gaussian squeezing of 6 and 7 dB available at the cluster state preparation. A major improvement by nonlinear feedforward appears for small Gaussian squeezing when considering finitely nonlinearly squeezed cubic state (18). The difference is even more pronounced for higher upperbound for Gaussian squeezing during optimization. Contrary, the regular teleportation does not gain much improvement with higher n -photon non-Gaussianity of the teleported state in the regime with 6 dB cluster state. The ideal nonlinear cubic phase measurement surpasses performance of all considered schemes. Altogether, when increasing the n -photon non-Gaussianity of the supporting states, the nonlinear feedforward starts manifesting advantage over teleportation, which lies in higher nonlinear squeezing at the output.

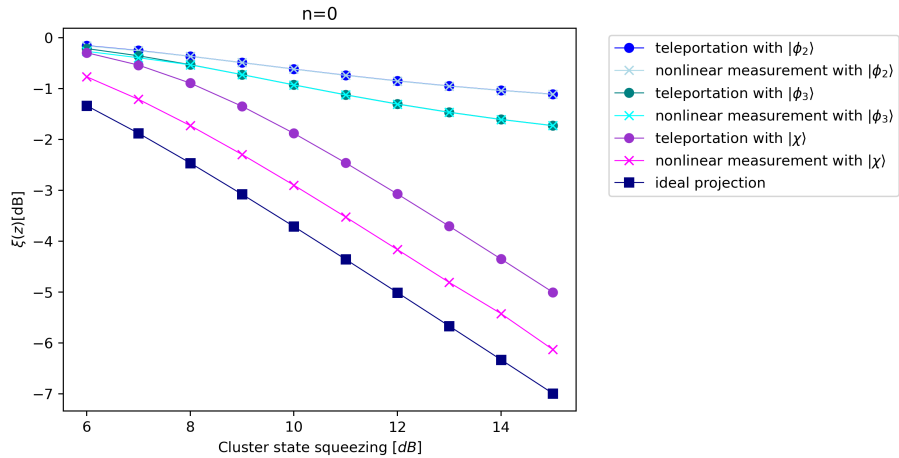


Figure 2: Nonlinear squeezing at the output mode, when the available Gaussian squeezing is limited to certain value [dB] during optimization. The two-mode cluster state is pure and optimized for each scheme. Output nonlinear squeezing is shown for regular and nonlinear teleportation of the superposition of vacuum state and single photon (20) and the state with 2-photon non-Gaussianity (21), both with optimized coefficients. Finally the results obtained with the finitely squeezed cubic state (18) and nonlinear cubic phase measurement.

Fig. 3 shows nonlinear squeezing transferred via the schemes when the cluster state is initially prepared not from a pure vacuum state but from thermal states that carry $n = 0.1$ additional vacuum fluctuations. The following optimization of the cluster state and the schemes is as for the previous plot within bounded Gaussian squeezing. The performance

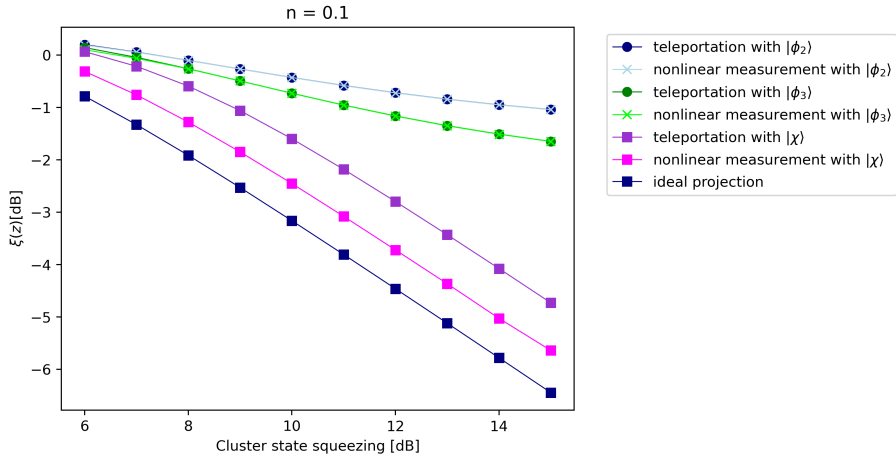


Figure 3: Nonlinear squeezing at the output mode, when the available Gaussian squeezing is limited to certain value [dB] during optimization. The two-mode cluster state carries $n = 0.1$ additional thermal noise.

for all schemes is negatively affected, however their relative comparison remains.

3.2 Probabilistic regime

Let us start with more detailed discussion of some cases presented in Fig. 2. To fully understand the role of the nonlinear feedforward, we will look at teleportation via 6 dB, 7 dB and 8 dB cluster state in a probabilistic regime, at all the measurement outcomes individually. We choose the two component superposition (20) for this analysis as it is close to experimental reality and the parameters of optical schemes and input states are taken from the optimized deterministic regime, thus they are the same as for which the results shown in Fig. 2 were obtained.

As the output mixture cover more states, the overall probability of success or obtaining such state increases, whereas the nonlinear squeezing diminishes, as can be seen in Fig. 4. This happens as a result of accepting less nonlinearly squeezed states to the mixture. As we increase the squeezing of cluster state, the advantage brought by the nonlinear feedforward vanishes. To see the behaviour as we decrease the cluster state squeezing we added a case of 4dB and 5dB cluster states, however it seems that from discussed cases, teleportation through the 6dB cluster state manifests the largest difference provided by the nonlinear feedforward.

We conclude our analysis by comparing performance of unity gain teleportation with and without the nonlinear feedforward. As the teleported state is considered the experimentally realistic two component superposition (20). Its specific form given by $u = 0.78977467$ is chosen such that the state is eigenstate of the operator O (5) restricted in Fock space to the subspace of dimension two. This approach ensures maximal nonlinear squeezing that can be obtained with superposition of vacuum and single photon state. The nonlinear squeezing is evaluated at this states' native cubicity. Thus a state with maximal nonlinear squeezing on a Fock subspace of dimension two is teleported and afterwards evaluation is done at its native cubicity before the teleportation. This setting leaves us with a single degree of freedom, χ in the nonlinear feedforward, which is optimized and yields $\chi = -0.219$ in the case of 6dB cluster state and $\chi = -0.130$ for 8dB cluster state.

Nonlinear squeezing shown in Fig. 6 is visibly enhanced by nonlinear feedforward and enables its detection even for probabilities for which the regular teleportation fails

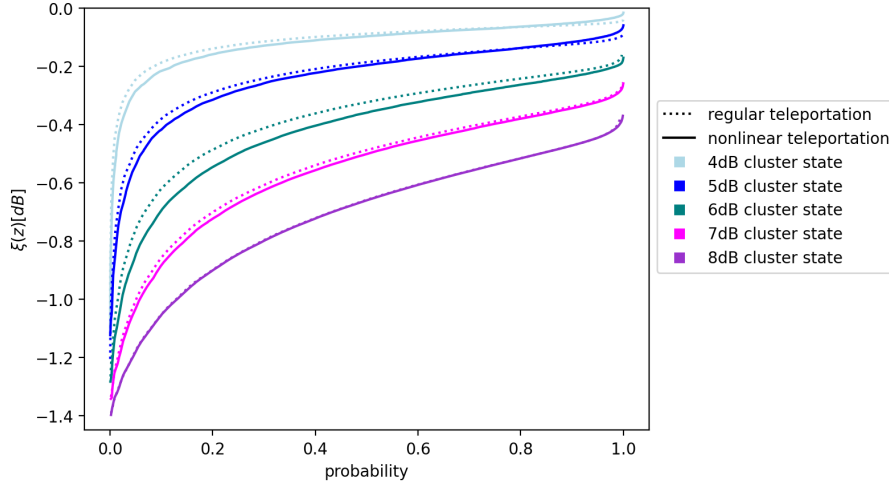


Figure 4: Nonlinear squeezing teleported by linear (dotted line) and nonlinear (solid line) teleportation. The input state and parameters of the optical scheme are optimized for the deterministic scenario. Quantum states depending on the measurement results with best nonlinear squeezing are aggregated up to a given probability.

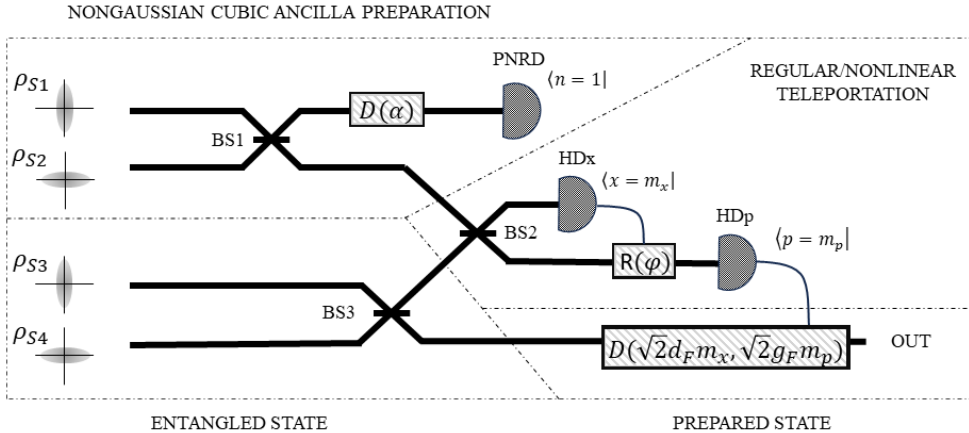


Figure 5: Scheme for conditioned regular/nonlinear teleportation including the preparation of the ancillary state.

to transfer any. We also introduced 25% losses to the ancillary state, that was present in its recent experimental preparation. The results are shown in dashed lines and again show advantage of the nonlinear teleportation with nonlinear feedforward. The optimal strength of the nonlinear feedforward is higher than for the ideal case, yielding $\chi = -0.250$ for 6dB cluster state and $\chi = -0.151$ for 8dB cluster state. A similar effect was recognized in decoherence of the nonlinear squeezing [17], where the native cubicity of the state increases with higher losses. In the presence of losses, the performances of teleportations through cluster states with 6 and 8 dB of Gaussian squeezing does not converge even for postselection on the best cases with vanishing probability.

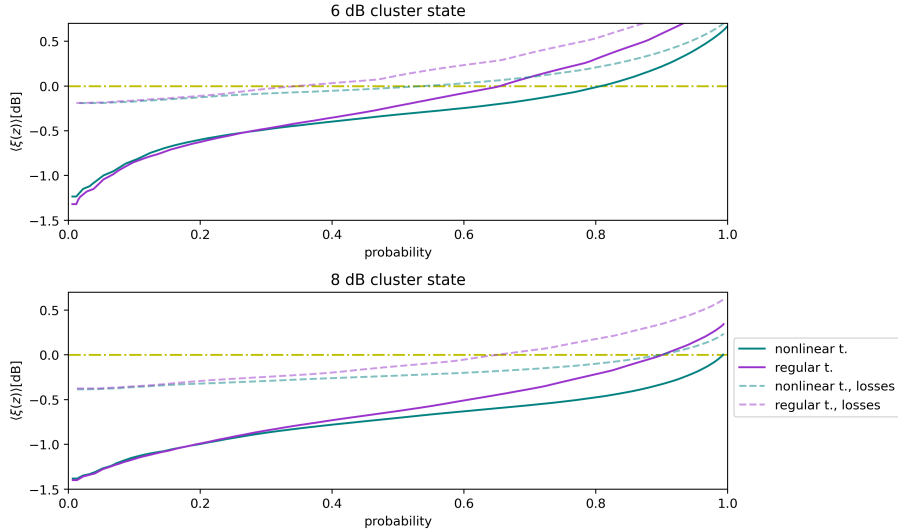


Figure 6: Nonlinear squeezing (16) produced by unity gain regular/nonlinear teleportation of an eigenstate of the operator O (5) conditioned on measurement results of the homodyne measurement with best results aggregated up to some probability and evaluated at native cubicity of the state before teleportation. The nonlinear teleportation and regular teleportation was simulated with two mode squeezed vacuum of 6 dB and 8 dB with (dashed lines) and without losses on the teleported state. Here it is assumed 25% losses [19]. In all cases the nonlinear squeezing firstly vanishes (the plot line crosses the dashed line of boundary 1) for regular teleportation.

4 Conclusion

The great remaining challenge of photonic continuous variable quantum computing remains in accompanying the rich multimode structure of Gaussian cluster states by non-Gaussian elements. As the basic mechanism of such cluster-state quantum computing serves the canonical teleportation protocol. Its performance, when non-Gaussianity is present, can be improved by adapting the measurement results processing.

We showed an improvement in the teleported nonlinear squeezing by involving currently experimentally tested nonlinear feedforward [36]. In a deterministic regime, the positive effect can be seen on the theoretical level of teleportation of the ideal cubic state. However in a probabilistic regime, when best results are postselected up to some probability, the improvement is observable even with current experimental resources in comparison to unity gain teleportation. Processing the measurement data during teleportation via classical nonlinear feedforward decreases the added amount of noise which can be seen by improved nonlinear squeezing at the output. The cubic nonlinear squeezing is a resource for measurement-based quantum computation [19, 36] and improving its amount that is transferred via teleportation increases the potential to chain and iterate computational steps as required by cluster computing.

The cubic nonlinearity itself is not currently experimentally available in travelling light, however a superposition of Fock states with nonlinear squeezing has already been prepared [19] as an alternative resource substituting the nonlinearity. Secondly, we show that in probabilistic regime the nonlinear teleportation equipped with nonlinear feedforward and currently experimentaly accessible state outperforms the unity gain linear teleportation through 6dB cluster state as is shown in Fig. 6. The advantage is thus in principle observable even with currently available nonlinearly squeezed state and appears by adjusting the classical part of the scheme consisting of nonlinear feedforward combined with

post-selection. The enhancement remains observable even in the presence of losses that accompanied the experimental preparation [19]. Our work is one of the first steps required to extend the presently Gaussian theory of cluster states into its final destination - non-Gaussian domain.

Acknowledgement

VK and PM acknowledge grant 22-08772S and RF grant 21-13491X of Czech Science Foundation. VK acknowledges the Quantera project CLUSSTAR (8C24003) of MEYS, Czech Republic. Project CLUSSTAR has received funding from the European Union's Horizon 2020 Research and Innovation Programme under Grant Agreements No. 731473 and No. 101017733 (QuantERA). PM acknowledges a grant from the Programme Johannes Amos Comenius under the Ministry of Education, Youth and Sports of the Czech Republic reg. no. CZ.02.01.01/00/22_008/0004649. VK, PM and RF also acknowledge Horizon Europe Research and Innovation Actions under Grant Agreement no. 101080173 (CLUSTEC). P.M. and R.F. acknowledge project CZ.02.01.010022 0080004649 (QUEENTEC) of EU and the Czech Ministry of Education, Youth and Sport. M.W. acknowledges funding from the Plan France 2030 through the project ANR-23-PETQ-0013. VK acknowledges project IGA-PrF-2024-008.

A Model in Heisenberg picture

In order to evaluate the nonlinear squeezing at the output of presented schemes we compute the transformation they generate in the Heisenberg picture. At first we describe the action of optical elements present in the schemes as quadrature transformations. The beam splitter generates a two-mode transformation on quadratures x_1, p_1, x_2 and p_2 of the form

$$\begin{aligned} x_1 &\rightarrow tx_1 + rx_2 \\ p_1 &\rightarrow tp_1 + rp_2 \\ x_2 &\rightarrow tx_2 - rx_1 \\ p_2 &\rightarrow tp_2 - rp_1, \end{aligned} \tag{23}$$

where t and r are transmissivity and reflectivity, respectively. Equation $t^2 + r^2 = 1$ holds.

Cubic nonlinearity acts on quadratures x and p as

$$\begin{aligned} x &\rightarrow x \\ p &\rightarrow p + \chi x^2, \end{aligned} \tag{24}$$

where we can see the appearance of the quadratic non-Gaussian term. Measurement of a quadrature q with outcome m can be expressed as

$$q = m, \tag{25}$$

provided, that the measurement outcome is used for feedforward to obtain independence on m .

Lets consider a general two-mode Gaussian state defined by quadratures x_A, p_A, x_B and p_B , where the A mode undergoes an ideal cubic nonlinearity followed by a homodyne measurement of p with measurement result proportional to

$$i_p = p_A + \chi x_A^2. \tag{26}$$

The measurement result is further used for p displacement of the mode B with gain g_p , yielding

$$\begin{aligned} x_B^{\text{out}} &= x_B \\ p_B^{\text{out}} &= p_B + g_p p_A + g_p \chi x_A^2 + z x_B^2. \end{aligned} \quad (27)$$

The nonlinear variance in (17) can be in this case expressed in terms of the quadratures of the two Gaussian modes A and B yields

$$\begin{aligned} \text{var}(p_B^{\text{out}} + z x_B^{\text{out}2}) &= \\ \text{var}(p_B) + 2g_p \text{cov}(p_A, p_B) + g_p^2 \text{var}(p_A) & \\ + 2\chi g_p \text{cov}(p_B, x_A^2) + 2z \text{cov}(p_B, x_B^2) & \\ + 2g_p^2 \chi \text{cov}(p_A, x_A^2) + 2g_p z \text{cov}(p_A, x_B^2) & \\ + g_p^2 \chi^2 \text{var}(x_A^2) + 2g_p \chi z \text{cov}(x_A^2, x_B^2) + z^2 \text{var}(x_B^2). & \end{aligned} \quad (28)$$

The schemes of measurement-induced nonlinearity and teleportation can be described by one model as they differ only by feedforwarded rotation parameterized by χ which can be switched off in the case of teleportation by setting $\chi = 0$. The measurement results of x -homodyne and p -homodyne in b) and c) of Fig. 1 yields

$$\begin{aligned} m_x &= tx_Q - r_x A \\ m_p &= \cos(\theta)(tp_A + rp_Q) - \sin(\theta)(tx_A + rx_Q), \end{aligned} \quad (29)$$

where quadratures with subscript Q are of the ancillary mode and with A of the first mode of the cluster state; θ depends on the measurement outcome of x -homodyne as

$$\theta = \sqrt{2}m_x\chi. \quad (30)$$

The measurement results are further feedforwarded to displacement on the output mode B with gains g_F and d_F

$$\begin{aligned} x_B^{\text{out}} &= d_F m_x \\ p_B^{\text{out}} &+ g_F m_p, \end{aligned} \quad (31)$$

where the superscript out denotes quadratures the the output of the scheme. We can now write the whole transformation

$$\begin{aligned} x_B^{\text{out}} &= x_B + d_F(tx_Q - rx_A) \\ p_B^{\text{out}} &= p_B + g_F \cos(\theta)(tp_A + rp_Q + \sqrt{2}\chi(tx_A + rx_Q)(rx_A - tx_Q)) \end{aligned} \quad (32)$$

Using this transformation and considering the second moments of modes A and B to be given by covariance matrices in (47), the variance of the operator $p_B^{\text{out}} + z x_B^{\text{out}2}$ can be expressed as follows. With shorthand notation of coefficients

$$\begin{aligned} A &= z \\ B &= 2d_F t z \\ C &= -2d_F r z \\ D &= -2d_F^2 r t z - \alpha \chi g_F t^2 + \alpha \chi g_F r^2 \\ E &= d_F^2 r^2 z + \alpha \chi g_F r t \\ F &= d_F^2 t^2 z - \alpha \chi g_F r t \end{aligned} \quad (33)$$

we can write

$$\begin{aligned}
& \text{var}(p_B^{\text{out}} + zx_B^{\text{out}2}) = \\
& \text{var}(p_B) + (\alpha g_{FT})^2 \text{var}(p_A) + (\alpha g_{FR})^2 \text{var}(p_Q) + 2\alpha g_{FT} \text{cov}(p_A, p_B) \\
& 2\{A\text{cov}(p_B, x_B^2) + B\text{cov}(p_B, x_Q x_B) + C\text{cov}(p_B, x_A x_B) + D\text{cov}(p_B, x_A x_Q) + E\text{cov}(p_B, x_A^2) \\
& + \alpha g_{FT}(\text{cov}(p_A, x_B^2) + B\text{cov}(p_A, x_Q x_B) + C\text{cov}(p_A, x_A x_B) + D\text{cov}(p_A, x_A x_Q) + E\text{cov}(p_A, x_A^2)) \\
& + \alpha g_{FR}(B\text{cov}(p_Q, x_Q x_B) + D\text{cov}(x_A x_Q, p_Q) + F\text{cov}(p_Q, x_Q^2)\}A^2 \text{var}(x_B^2) + 2AB\text{cov}(x_B^2, x_Q x_B) + \\
& 2AC\text{cov}(x_B^2, x_A x_B) + 2AD\text{cov}(x_B^2, x_A x_Q) + 2AE\text{cov}(x_A^2, x_B^2) + B^2 \text{var}(x_Q x_B) \\
& + 2BC\text{cov}(x_Q x_B, x_A x_B)(-2drz) + 2BD\text{cov}(x_Q x_B, x_A x_Q) + 2BE\text{cov}(x_Q x_B, x_A^2) + \\
& 2BF\text{cov}(x_Q x_B, x_Q^2) + F^2 \text{var}(x_Q^2)2FC\text{cov}(x_Q^2, x_A x_B) + 2FD\text{cov}(x_Q^2, x_A x_Q) + 2FE\text{cov}(x_Q^2, x_A^2) + \\
& C^2 \text{var}(x_A x_B) + 2CD\text{cov}(x_A x_B, x_A x_Q) + 2CE\text{cov}(x_A x_B, x_A^2) + \\
& D^2 \text{var}(x_A x_Q) + 2DE\text{cov}(x_A x_Q, x_A^2) + E^2 \text{var}(x_A^2).
\end{aligned} \tag{34}$$

The Gaussianity of the cluster state can be used for expressing the whole expression in terms appearing in covariance matrix of the modes A and B. For the more complex moments involving more than two quadratures, we use the generalized Stein's lemma for multivariate Gaussian distributions of a random variable \vec{X} with mean values $\vec{\mu}$ [24]

$$E(g(X)X_i) = \mu_i E(g(X)) + \sum_j C_{ij} E(\partial_j g(X)). \tag{35}$$

The Stein's lemma cannot be used generally for computation of quantum moments. It is necessary, that those moments are Weyl symmetrical.

$$\begin{aligned}
\text{cov}(p_B, x_B^2) &= 2 \langle x_B \rangle \text{cov}(x_P, p_B) \\
\text{cov}(p_B, x_Q x_B) &= 0 \text{ due to } \langle x_Q \rangle = 0 \\
\text{cov}(p_B, x_A x_Q) &= \langle x_Q \rangle \text{cov}(x_A, p_B) = 0 \\
\text{cov}(p_B, x_A^2) &= 2 \langle x_A \rangle \text{cov}(x_A, p_B) \\
\text{cov}(p_A, x_B^2) &= 2 \langle x_B \rangle \text{cov}(x_B, p_A) \\
\text{cov}(p_A, x_Q x_B) &= 0 \\
\text{cov}(p_A, x_A x_Q) &= 0 \\
\text{cov}(p_A, x_A^2) &= 2 \langle x_A \rangle \text{cov}(x_A, p_A) \\
\text{cov}(p_Q, x_Q x_B) &= \langle x_B \rangle \text{cov}(x_Q, p_Q) \\
\text{cov}(p_Q, x_A x_Q) &= \langle x_A \rangle \text{cov}(x_Q, p_Q) \\
\text{cov}(p_B, x_A x_B) &= \langle x_B \rangle \text{cov}(x_A, p_B) + \langle x_A \rangle \text{cov}(x_B, p_B) \\
\text{cov}(p_A, x_A x_B) &= \langle x_A \rangle \text{cov}(x_B, p_A) + \langle x_B \rangle \text{cov}(x_A, p_A) \\
\text{cov}(x_B^2, x_Q x_B) &= 0 \\
\text{cov}(x_B^2, x_A x_B) &= \langle x_A \rangle \langle x_B \rangle^3 + 3\text{cov}(x_A, x_B) \langle x_B^2 \rangle + \\
&3\text{var}(x_B) \langle x_A \rangle \langle x_B \rangle + 3\text{var}(x_B) \text{cov}(x_A, x_B) - (\text{cov}(x_A, x_B) + \langle x_A \rangle \langle x_B \rangle)(\text{var}(x_B) + \langle x_B \rangle^2) \\
&= 2 \langle x_B \rangle^2 \text{cov}(x_A, x_B) + 2 \langle x_A \rangle \langle x_B \rangle \text{var}(x_B) + 2\text{var}(x_B) \text{cov}(x_A, x_B) \\
\text{cov}(x_B^2, x_A x_Q) &= 0 \\
\text{var}(x_Q x_B) &= \langle x_Q^2 \rangle (\text{var}(x_B) + \langle x_B \rangle^2) \\
\text{cov}(x_A^2, x_B^2) &= 4\text{cov}(x_A, x_B) \langle x_A \rangle \langle x_B \rangle + 2\text{cov}(x_A, x_B)^2 \\
\text{cov}(x_Q x_B, x_A x_B) &= \langle x_Q \rangle \langle x_B \rangle \text{cov}(x_A, x_B) + \langle x_Q \rangle \langle x_A \rangle \text{cov}(x_B, x_B) \\
\text{cov}(x_Q x_B, x_A^2) &= 0 \\
\text{cov}(x_Q x_B, x_Q^2) &= \langle x_B \rangle \text{cov}(x_Q, x_Q^2) \\
\text{cov}(x_Q^2, x_A x_B) &= 0 \\
\text{cov}(x_Q^2, x_A x_Q) &= \langle x_A \rangle \text{cov}(x_Q, x_Q^2) \\
\text{cov}(x_Q^2, x_A^2) &= 0 \\
\text{var}(x_A x_B) &= \text{var}(x_A) \langle x_B \rangle^2 + 2\text{cov}(x_A, x_B) \langle x_A \rangle \langle x_B \rangle + \\
&\text{var}(x_B) \langle x_A \rangle^2 + \text{cov}(x_A, x_B)^2 + \text{var}(x_A) \text{var}(x_B) \\
\text{cov}(x_A x_B, x_A x_Q) &= 0 \\
\text{cov}(x_A x_B, x_A^2) &= \langle x_B \rangle \langle x_A \rangle^3 + 3\text{cov}(x_A, x_B) \langle x_A \rangle^2 + \\
&3\text{var}(x_A) \langle x_A \rangle \langle x_B \rangle + 3\text{var}(x_A) \text{cov}(x_A, x_B) - (\text{cov}(x_A, x_B) + \\
&\langle x_A \rangle \langle x_B \rangle)(\text{var}(x_A) + \langle x_A \rangle^2) \\
&= 2(\text{var}(x_A) \text{cov}(x_A, x_B) + \text{cov}(x_A, x_B) \langle x_A \rangle^2 + \text{var}(x_A) \langle x_A \rangle \langle x_B \rangle) \\
\text{var}(x_A x_Q) &= \langle x_Q^2 \rangle (\text{var}(x_A) + \langle x_A \rangle^2) \\
\text{cov}(x_A x_Q, x_A^2) &= 0 \\
\text{var}(x_A^2) &= 4\text{var}(x_A) \langle x_A \rangle^2 + 2\text{var}(x_A)^2 \\
\text{var}(x_B^2) &= 4\text{var}(x_B) \langle x_B \rangle^2 + 2\text{var}(x_B)^2
\end{aligned} \tag{36}$$

Additionally, for the finitely nonlinearly squeezed state (18) and its approximation (20) holds

$$\begin{aligned} \text{cov}(x_Q, p_Q) &= 0 \\ \langle x_Q \rangle &= 0 \\ \text{cov}(x_Q, x_Q^2) &= 0 \\ \langle x_Q^2 \rangle &= \frac{1}{2g} \end{aligned} \tag{37}$$

$$\langle x_Q^2 \rangle = \frac{3}{2} - u^2 \tag{38}$$

$$\begin{aligned} \text{cov}(x_Q, p'_Q) &= 0 \\ \langle x_Q \rangle &= 0 \\ \text{cov}(x_Q, x_Q^2) &= 0 \\ \langle x_Q^2 \rangle &= \frac{3}{2} - u^2 \end{aligned} \tag{39}$$

$$\begin{aligned} \text{var}(p_Q) &= 2u^4 - 3u^2 + \frac{3}{2} \\ \text{var}(x_Q^2) &= \frac{3}{2} - u^4 \\ \text{cov}(x_Q^2, p_Q) &= \sqrt{2(1-u^2)}u(u^2-1). \end{aligned} \tag{40}$$

B Parametrization of the general two-mode cluster state and its optimization

For the two-mode cluster state we considered a general Gaussian state which is prepared from a thermal state ρ_T as

$$\begin{aligned} &R_1(\phi_1)R_2(\phi_2)U_{\text{BS}}R_1(\phi)S_1(r_1)S_2(r_2)\rho_T \otimes \\ &\rho_T S_2(r_2)^\dagger S_1(r_1)^\dagger R_1(\phi)^\dagger U_{\text{BS}}^\dagger R_2(\phi_2)^\dagger R_1(\phi_1)^\dagger, \end{aligned} \tag{41}$$

where $R_i(\phi)$, $S_i(r)$ are rotation and Gaussian squeezing acting on the i -th mode and U_{BS} is a unitary transformation of beam splitter. Initial thermal state has covariance matrix

$$\gamma_{\text{in}} = \begin{pmatrix} \frac{1}{2}(1+n) & 0 & 0 & 0 \\ 0 & \frac{1}{2}(1+n) & 0 & 0 \\ 0 & 0 & \frac{1}{2}(1+n) & 0 \\ 0 & 0 & 0 & \frac{1}{2}(1+n). \end{pmatrix} \tag{42}$$

Being a pure state for $n = 0$ and having n times added vacuum noise if thermal. The symplectic transformation representing squeezing yields

$$S = \begin{pmatrix} \frac{1}{g_1} & 0 & 0 & 0 \\ 0 & g_1 & 0 & 0 \\ 0 & 0 & g_2 & 0 \\ 0 & 0 & 0 & \frac{1}{g_2} \end{pmatrix}, \tag{43}$$

where $g = \exp(r/2)$. Symplectic transformation of beam splitter

$$S_{BS} = \begin{pmatrix} t & 0 & r & 0 \\ 0 & t & 0 & r \\ -r & 0 & t & 0 \\ 0 & -r & 0 & t \end{pmatrix}, \quad (44)$$

where t is transmissivity and $t^2 + r^2 = 1$ holds. Rotation of the first mode is described as

$$R_1 = \begin{pmatrix} \cos(\phi) & \sin(\phi) & 0 & 0 \\ -\sin(\phi) & \cos(\phi) & 0 & 0 \\ 0 & 0 & 1 & 0 \\ 0 & 0 & 0 & 1 \end{pmatrix}. \quad (45)$$

And finally, the rotation of both modes yields

$$R_{12} = \begin{pmatrix} \cos(\phi_1) & \sin(\phi_1) & 0 & 0 \\ -\sin(\phi_1) & \cos(\phi_1) & 0 & 0 \\ 0 & 0 & \cos(\phi_2) & \sin(\phi_2) \\ 0 & 0 & -\sin(\phi_2) & \cos(\phi_2) \end{pmatrix}. \quad (46)$$

The overall covariance matrix of the two-mode state is then computed as

$$\gamma = R_{12} S_{BS} R_1 S \gamma_{in} S^T R_1^T S_{BS}^T R_{12}^T \quad (47)$$

C Optimization of the cluster state

We performed numerical optimization with `scipy.optimize minimize` modul with 400-460 randomly chosen initial states with covariance matrix (47). The initial conditions were chosen within a range given by the upper bound on the maximal Gaussian squeezing, an interval ± 10 for mean values of x quadratures, cubicities χ and z and gains in an interval ± 2 and arbitrary rotations.

References

- [1] Warit Asavanant, Kota Nakashima, Yu Shiozawa, Jun-Ichi Yoshikawa, and Akira Furusawa. Generation of highly pure schrödinger’s cat states and real-time quadrature measurements via optical filtering. *Opt. Express*, 25(26):32227–32242, Dec 2017. DOI: [10.1364/OE.25.032227](https://doi.org/10.1364/OE.25.032227). URL <https://opg.optica.org/oe/abstract.cfm?URI=oe-25-26-32227>.
- [2] Masashi Ban, Masahide Sasaki, and Masahiro Takeoka. Continuous variable teleportation as a generalized thermalizing quantum channel. *Journal of Physics A: Mathematical and General*, 35(28):L401, jul 2002. DOI: [10.1088/0305-4470/35/28/102](https://doi.org/10.1088/0305-4470/35/28/102). URL <https://dx.doi.org/10.1088/0305-4470/35/28/102>.
- [3] Hugo Benichi, Shuntaro Takeda, Noriyuki Lee, and Akira Furusawa. Quantum teleportation of nonclassical wave packets: An effective multimode theory. *Phys. Rev. A*, 84:012308, Jul 2011. DOI: [10.1103/PhysRevA.84.012308](https://doi.org/10.1103/PhysRevA.84.012308). URL <https://link.aps.org/doi/10.1103/PhysRevA.84.012308>.
- [4] Samuel L. Braunstein. Squeezing as an irreducible resource. *Phys. Rev. A*, 71:055801, May 2005. DOI: [10.1103/PhysRevA.71.055801](https://doi.org/10.1103/PhysRevA.71.055801). URL <https://link.aps.org/doi/10.1103/PhysRevA.71.055801>.

[5] Ulysse Chabaud and Mattia Walschaers. Resources for bosonic quantum computational advantage. *Phys. Rev. Lett.*, 130:090602, Mar 2023. DOI: [10.1103/PhysRevLett.130.090602](https://doi.org/10.1103/PhysRevLett.130.090602). URL <https://link.aps.org/doi/10.1103/PhysRevLett.130.090602>.

[6] Ulysse Chabaud, Damian Markham, and Frédéric Grosshans. Stellar representation of non-gaussian quantum states. *Physical Review Letters*, 124(6), feb 2020. DOI: [10.1103/physrevlett.124.063605](https://doi.org/10.1103/physrevlett.124.063605). URL <https://doi.org/10.1103/physrevlett.124.063605>.

[7] Radim Filip, Petr Marek, and Ulrik L. Andersen. Measurement-induced continuous-variable quantum interactions. *Phys. Rev. A*, 71:042308, Apr 2005. DOI: [10.1103/PhysRevA.71.042308](https://doi.org/10.1103/PhysRevA.71.042308). URL <https://link.aps.org/doi/10.1103/PhysRevA.71.042308>.

[8] Akira Furusawa, Jens Lykke Sørensen, Samuel L Braunstein, Christopher A Fuchs, H Jeff Kimble, and Eugene S Polzik. Unconditional quantum teleportation. *Science*, 282(5389):706–709, 1998. ISSN 0036-8075. DOI: [10.1126/science.282.5389.706](https://doi.org/10.1126/science.282.5389.706). URL <https://science.scienmag.org/content/282/5389/706>.

[9] Maria Fuwa, Shunsuke Toba, Shuntaro Takeda, Petr Marek, Ladislav Mišta, Radim Filip, Peter van Loock, Jun-ichi Yoshikawa, and Akira Furusawa. Noiseless conditional teleportation of a single photon. *Phys. Rev. Lett.*, 113:223602, Nov 2014. DOI: [10.1103/PhysRevLett.113.223602](https://doi.org/10.1103/PhysRevLett.113.223602). URL <https://link.aps.org/doi/10.1103/PhysRevLett.113.223602>.

[10] Shohini Ghose and Barry C. Sanders. Non-gaussian ancilla states for continuous variable quantum computation via gaussian maps. *Journal of Modern Optics*, 54(6): 855–869, 2007. DOI: [10.1080/09500340601101575](https://doi.org/10.1080/09500340601101575). URL <https://doi.org/10.1080/09500340601101575>.

[11] Daniel Gottesman, Alexei Kitaev, and John Preskill. Encoding a qubit in an oscillator. *Phys. Rev. A*, 64:012310, Jun 2001. DOI: [10.1103/PhysRevA.64.012310](https://doi.org/10.1103/PhysRevA.64.012310). URL <https://link.aps.org/doi/10.1103/PhysRevA.64.012310>.

[12] Craig S. Hamilton, Regina Kruse, Linda Sansoni, Sonja Barkhofen, Christine Silberhorn, and Igor Jex. Gaussian boson sampling. *Phys. Rev. Lett.*, 119:170501, Oct 2017. DOI: [10.1103/PhysRevLett.119.170501](https://doi.org/10.1103/PhysRevLett.119.170501). URL <https://link.aps.org/doi/10.1103/PhysRevLett.119.170501>.

[13] Timo Hillmann, Fernando Quijandría, Arne L. Grimsmo, and Giulia Ferrini. Performance of teleportation-based error-correction circuits for bosonic codes with noisy measurements. *PRX Quantum*, 3:020334, May 2022. DOI: [10.1103/PRXQuantum.3.020334](https://doi.org/10.1103/PRXQuantum.3.020334). URL <https://link.aps.org/doi/10.1103/PRXQuantum.3.020334>.

[14] K. Huang, H. Le Jeannic, J. Ruaudel, V. B. Verma, M. D. Shaw, F. Marsili, S. W. Nam, E Wu, H. Zeng, Y.-C. Jeong, R. Filip, O. Morin, and J. Laurat. Optical synthesis of large-amplitude squeezed coherent-state superpositions with minimal resources. *Phys. Rev. Lett.*, 115:023602, Jul 2015. DOI: [10.1103/PhysRevLett.115.023602](https://doi.org/10.1103/PhysRevLett.115.023602). URL <https://link.aps.org/doi/10.1103/PhysRevLett.115.023602>.

[15] Toshiki Ide, Holger F. Hofmann, Takayoshi Kobayashi, and Akira Furusawa. Continuous-variable teleportation of single-photon states. *Phys. Rev. A*, 65:012313, Dec 2001. DOI: [10.1103/PhysRevA.65.012313](https://doi.org/10.1103/PhysRevA.65.012313). URL <https://link.aps.org/doi/10.1103/PhysRevA.65.012313>.

[16] Hanna Le Jeannic, Adrien Cavaillès, Kun Huang, Radim Filip, and Julien Laurat. Slowing quantum decoherence by squeezing in phase space. *Phys. Rev. Lett.*, 120: 073603, Feb 2018. DOI: [10.1103/PhysRevLett.120.073603](https://doi.org/10.1103/PhysRevLett.120.073603). URL <https://link.aps.org/doi/10.1103/PhysRevLett.120.073603>.

[17] Vojtěch Kala, Radim Filip, and Petr Marek. Cubic nonlinear squeezing and its de-coherence. *Opt. Express*, 30(17):31456–31471, Aug 2022. DOI: 10.1364/OE.464759. URL <https://opg.optica.org/oe/abstract.cfm?URI=oe-30-17-31456>.

[18] Shunya Konno, Warit Asavanant, Kosuke Fukui, Atsushi Sakaguchi, Fumiya Hanamura, Petr Marek, Radim Filip, Jun-ichi Yoshikawa, and Akira Furusawa. Non-clifford gate on optical qubits by nonlinear feedforward. *Phys. Rev. Res.*, 3:043026, Oct 2021. DOI: 10.1103/PhysRevResearch.3.043026. URL <https://link.aps.org/doi/10.1103/PhysRevResearch.3.043026>.

[19] Shunya Konno, Atsushi Sakaguchi, Warit Asavanant, Hisashi Ogawa, Masaya Kobayashi, Petr Marek, Radim Filip, Jun-ichi Yoshikawa, and Akira Furusawa. Non-linear squeezing for measurement-based non-gaussian operations in time domain. *Phys. Rev. Applied*, 15:024024, Feb 2021. DOI: 10.1103/PhysRevApplied.15.024024. URL <https://link.aps.org/doi/10.1103/PhysRevApplied.15.024024>.

[20] Shunya Konno, Warit Asavanant, Fumiya Hanamura, Hironari Nagayoshi, Kosuke Fukui, Atsushi Sakaguchi, Ryuhoh Ide, Fumihiro China, Masahiro Yabuno, Shigehito Miki, Hirotaka Terai, Kan Takase, Mamoru Endo, Petr Marek, Radim Filip, Peter van Loock, and Akira Furusawa. Logical states for fault-tolerant quantum computation with propagating light. *Science*, 383(6680):289–293, 2024. DOI: 10.1126/science.adk7560. URL <https://www.science.org/doi/abs/10.1126/science.adk7560>.

[21] Lukáš Lachman, Ivo Straka, Josef Hloušek, Miroslav Ježek, and Radim Filip. Faithful hierarchy of genuine n -photon quantum non-gaussian light. *Phys. Rev. Lett.*, 123: 043601, Jul 2019. DOI: 10.1103/PhysRevLett.123.043601. URL <https://link.aps.org/doi/10.1103/PhysRevLett.123.043601>.

[22] Mikkel V. Larsen, Xueshi Guo, Casper R. Breum, Jonas S. Neergaard-Nielsen, and Ulrik L. Andersen. Deterministic generation of a two-dimensional cluster state. *Science*, 366(6463):369–372, 2019. DOI: 10.1126/science.aay4354. URL <https://www.science.org/doi/abs/10.1126/science.aay4354>.

[23] Noriyuki Lee, Hugo Benichi, Yuishi Takeno, Shuntaro Takeda, James Webb, Elanor Huntington, and Akira Furusawa. Teleportation of nonclassical wave packets of light. *Science*, 332(6027):330–333, 2011. DOI: 10.1126/science.1201034. URL <https://www.science.org/doi/abs/10.1126/science.1201034>.

[24] Jun S. Liu. Siegel’s formula via stein’s identities. *Statistics & Probability Letters*, 21(3):247–251, 1994. ISSN 0167-7152. DOI: [https://doi.org/10.1016/0167-7152\(94\)90121-X](https://doi.org/10.1016/0167-7152(94)90121-X). URL <https://www.sciencedirect.com/science/article/pii/016771529490121X>.

[25] Seth Lloyd and Samuel L. Braunstein. Quantum computation over continuous variables. *Phys. Rev. Lett.*, 82:1784–1787, Feb 1999. DOI: 10.1103/PhysRevLett.82.1784. URL <https://link.aps.org/doi/10.1103/PhysRevLett.82.1784>.

[26] Andrea Mari and Jens Eisert. Positive wigner functions render classical simulation of quantum computation efficient. *Phys. Rev. Lett.*, 109:230503, Dec 2012. DOI: 10.1103/PhysRevLett.109.230503. URL <https://link.aps.org/doi/10.1103/PhysRevLett.109.230503>.

[27] Mohamed F. Melalkia, Tecla Gabbrielli, Antoine Petitjean, Léandre Brunel, Alessandro Zavatta, Sébastien Tanzilli, Jean Etesse, and Virginia D’Auria. Plug-and-play generation of non-gaussian states of light at a telecom wavelength. *Opt. Express*, 30(25):45195–45201, Dec 2022. DOI: 10.1364/OE.465980. URL <https://opg.optica.org/oe/abstract.cfm?URI=oe-30-25-45195>.

[28] Nicolas C. Menicucci. Fault-tolerant measurement-based quantum computing

with continuous-variable cluster states. *Phys. Rev. Lett.*, 112:120504, Mar 2014. DOI: 10.1103/PhysRevLett.112.120504. URL <https://link.aps.org/doi/10.1103/PhysRevLett.112.120504>.

[29] Nicolas C. Menicucci, Peter van Loock, Mile Gu, Christian Weedbrook, Timothy C. Ralph, and Michael A. Nielsen. Universal quantum computation with continuous-variable cluster states. *Phys. Rev. Lett.*, 97:110501, Sep 2006. DOI: 10.1103/PhysRevLett.97.110501. URL <https://link.aps.org/doi/10.1103/PhysRevLett.97.110501>.

[30] Ladislav Mišta, Radim Filip, and Akira Furusawa. Continuous-variable teleportation of a negative wigner function. *Phys. Rev. A*, 82:012322, Jul 2010. DOI: 10.1103/PhysRevA.82.012322. URL <https://link.aps.org/doi/10.1103/PhysRevA.82.012322>.

[31] Kazunori Miyata, Hisashi Ogawa, Petr Marek, Radim Filip, Hidehiro Yonezawa, Jun-ichi Yoshikawa, and Akira Furusawa. Implementation of a quantum cubic gate by an adaptive non-gaussian measurement. *Phys. Rev. A*, 93:022301, Feb 2016. DOI: 10.1103/PhysRevA.93.022301. URL <https://link.aps.org/doi/10.1103/PhysRevA.93.022301>.

[32] Jeremy L. O’Brien. Optical quantum computing. *Science*, 318(5856):1567–1570, 2007. ISSN 0036-8075. DOI: 10.1126/science.1142892. URL <https://science.scienmag.org/content/318/5856/1567>.

[33] Hisashi Ogawa, Hideaki Ohdan, Kazunori Miyata, Masahiro Taguchi, Kenzo Makino, Hidehiro Yonezawa, Jun-ichi Yoshikawa, and Akira Furusawa. Real-time quadrature measurement of a single-photon wave packet with continuous temporal-mode matching. *Phys. Rev. Lett.*, 116:233602, Jun 2016. DOI: 10.1103/PhysRevLett.116.233602. URL <https://link.aps.org/doi/10.1103/PhysRevLett.116.233602>.

[34] Alexei Ourjoumtsev, Rosa Tualle-Brouri, Julien Laurat, and Philippe Grangier. Generating optical schrödinger kittens for quantum information processing. *Science*, 312(5770):83–86, 2006. ISSN 0036-8075. DOI: 10.1126/science.1122858. URL <https://science.scienmag.org/content/312/5770/83>.

[35] Stefano Pirandola, Jens Eisert, Christian Weedbrook, A. Furusawa, and S. L. Braunstein. Advances in quantum teleportation. *Nat. Phot.*, 9:641–652, 2015. DOI: 10.1038/nphoton.2015.154.

[36] Atsushi Sakaguchi, Shunya Konno, Fumiya Hanamura, Warit Asavanant, Kan Takase, Hisashi Ogawa, Petr Marek, Radim Filip, Jun-ichi Yoshikawa, Elanor Huntington, Hidehiro Yonezawa, and Akira Furusawa. Nonlinear feedforward enabling quantum computation. *Nature Communications*, 14(1):3817, Jul 2023. ISSN 2041-1723. DOI: 10.1038/s41467-023-39195-w. URL <https://doi.org/10.1038/s41467-023-39195-w>.

[37] Seckin Sefi, Petr Marek, and Radim Filip. Deterministic multi-mode nonlinear coupling for quantum circuits. *New Journal of Physics*, 21(6):063018, jun 2019. DOI: 10.1088/1367-2630/ab246d. URL <https://doi.org/10.1088/1367-2630/ab246d>.

[38] Ryuji Takagi and Quntao Zhuang. Convex resource theory of non-gaussianity. *Phys. Rev. A*, 97:062337, Jun 2018. DOI: 10.1103/PhysRevA.97.062337. URL <https://link.aps.org/doi/10.1103/PhysRevA.97.062337>.

[39] Kan Takase, Kosuke Fukui, Akito Kawasaki, Warit Asavanant, Mamoru Endo, Jun-ichi Yoshikawa, Peter van Loock, and Akira Furusawa. Gottesman-kitaev-preskill qubit synthesizer for propagating light. *npj Quantum Information*, 9(1):98, Oct 2023. ISSN 2056-6387. DOI: 10.1038/s41534-023-00772-y. URL <https://doi.org/10.1038/s41534-023-00772-y>.

[40] Shuntaro Takeda, Takahiro Mizuta, Maria Fuwa, Hidehiro Yonezawa, Peter van Loock,

and Akira Furusawa. Gain tuning for continuous-variable quantum teleportation of discrete-variable states. *Phys. Rev. A*, 88:042327, Oct 2013. DOI: [10.1103/PhysRevA.88.042327](https://doi.org/10.1103/PhysRevA.88.042327). URL <https://link.aps.org/doi/10.1103/PhysRevA.88.042327>.

[41] Masahiro Takeoka, Masashi Ban, and Masahide Sasaki. Quantum channel of continuous variable teleportation and nonclassicality of quantum states. *Journal of Optics B: Quantum and Semiclassical Optics*, 4(2):114, feb 2002. DOI: [10.1088/1464-4266/4/2/306](https://doi.org/10.1088/1464-4266/4/2/306). URL <https://dx.doi.org/10.1088/1464-4266/4/2/306>.

[42] Masahiro Takeoka, Jonas Neergaard-Nielsen, M. Takeuchi, Kentaro Wakui, H. Takahashi, K. Hayasaka, and M. Sasaki. Engineering of optical continuous-variable qubits via displaced photon subtraction: multimode analysis. *Journal of Modern Optics*, 58(3-4):266–275, 2011. DOI: [10.1080/09500340.2010.533205](https://doi.org/10.1080/09500340.2010.533205). URL <https://doi.org/10.1080/09500340.2010.533205>.

[43] Johannes Tiedau, Tim J. Bartley, Georg Harder, Adriana E. Lita, Sae Woo Nam, Thomas Gerrits, and Christine Silberhorn. Scalability of parametric down-conversion for generating higher-order fock states. *Phys. Rev. A*, 100:041802, Oct 2019. DOI: [10.1103/PhysRevA.100.041802](https://doi.org/10.1103/PhysRevA.100.041802). URL <https://link.aps.org/doi/10.1103/PhysRevA.100.041802>.

[44] Alfred U’Ren, Christine Silberhorn, Konrad Banaszek, and Ian Walmsley. Efficient conditional preparation of high-fidelity single photon states for fiber-optic quantum networks. *Physical review letters*, 93:093601, 09 2004. DOI: [10.1103/PhysRevLett.93.093601](https://doi.org/10.1103/PhysRevLett.93.093601).

[45] Šimon Bräuer and Petr Marek. Generation of quantum states with nonlinear squeezing by kerr nonlinearity. *Opt. Express*, 29(14):22648–22658, Jul 2021. DOI: [10.1364/OE.427637](https://doi.org/10.1364/OE.427637). URL <http://www.opticsexpress.org/abstract.cfm?URI=oe-29-14-22648>.

[46] Mattia Walschaers and Nicolas Treps. Remote generation of wigner negativity through einstein-podolsky-rosen steering. *Phys. Rev. Lett.*, 124:150501, Apr 2020. DOI: [10.1103/PhysRevLett.124.150501](https://doi.org/10.1103/PhysRevLett.124.150501). URL <https://link.aps.org/doi/10.1103/PhysRevLett.124.150501>.

[47] Blayne W. Walshe, Ben Q. Baragiola, Rafael N. Alexander, and Nicolas C. Menicucci. Continuous-variable gate teleportation and bosonic-code error correction. *Phys. Rev. A*, 102:062411, Dec 2020. DOI: [10.1103/PhysRevA.102.062411](https://doi.org/10.1103/PhysRevA.102.062411). URL <https://link.aps.org/doi/10.1103/PhysRevA.102.062411>.

[48] Shota Yokoyama, Ryuji Ukai, Seiji C. Armstrong, Chanond Sornphiphatphong, Toshiyuki Kaji, Shigenari Suzuki, Jun ichi Yoshikawa, Hidehiro Yonezawa, Nicolas C. Menicucci, and Akira Furusawa. Ultra-large-scale continuous-variable cluster states multiplexed in the time domain. *Nat. Phot.*, 7:982–986, 2013. DOI: [10.1038/nphoton.2013.287](https://doi.org/10.1038/nphoton.2013.287).

[49] Mitsuyoshi Yukawa, Kazunori Miyata, Takahiro Mizuta, Hidehiro Yonezawa, Petr Marek, Radim Filip, and Akira Furusawa. Generating superposition of up-to three photons for continuous variable quantum information processing. *Optics Express*, 21 (5):5529, feb 2013. DOI: [10.1364/oe.21.005529](https://doi.org/10.1364/oe.21.005529). URL <https://doi.org/10.1364/oe.21.005529>.

[50] Alessandro Zavatta, Silvia Viciani, and Marco Bellini. Quantum-to-classical transition with single-photon-added coherent states of light. *Science*, 306(5696):660–662, 2004. ISSN 0036-8075. DOI: [10.1126/science.1103190](https://doi.org/10.1126/science.1103190). URL <https://science.sciencemag.org/content/306/5696/660>.

[51] Jie Zhao, Hao Jeng, Lorcán O. Conlon, Spyros Tserkis, Biveen Shajilal, Kui Liu, Timothy C. Ralph, Syed M. Assad, and Ping Koy Lam. Enhancing quantum tele-

portation efficacy with noiseless linear amplification. *Nature Communications*, 14 (1):4745, Aug 2023. ISSN 2041-1723. DOI: 10.1038/s41467-023-40438-z. URL <https://doi.org/10.1038/s41467-023-40438-z>.